# Contrast Enhancement for Liver Tumor Identification

Hanung Adi Nugroho[1,2], Dani Ihtatho[1] and Hermawan Nugroho[1]

July 7, 2008

[1]Department of Electrical and Electronic Engineering, Universiti Teknologi PETRONAS
Bandar Seri Iskandar, 31750 Tronoh, Perak Darul Ridzuan, Malaysia
[2]Department of Electrical Engineering, Gadjah Mada University
Jogjakarta, Indonesia

**Abstract**

In CT images, tumors located in a liver are generally identified by intensity difference between tumor and liver. The intensity of the tumor can be lower and or higher than that of the liver. However, the main problem of liver tumor detection from is related to low contrast between tumor and liver intensities. Tumor sometimes presents in a very small dimension and makes the detection even more difficult. In this work, we focus on contrast enhancement of CT images containing liver and tumor based on the histogram processing as a necessary preprocessing for liver tumor identification. Results show that using our proposed method, the contrast of the CT images can be enhanced and results in relatively accurate identification of tumors in the liver.

*Keyword: liver tumor, contrast enhancement, histogram processing*

## Contents



.

## 1 Introduction

Cancer is associated with substantial morbidity and mortality. Currently, in United States one in four deaths is due to cancer [1]. It is known that cancer can affect different body system, such as digestive system, respiratory system, soft tissues and skin, bones and joints, genital system, urinary system, eye and endocrine system. Liver cancer is one type of cancer. One concerning

fact about liver cancer is that its mortality rate. While other cancer cases are declining, liver cancer is increasing exponentially from 1990 to 2003. From the report, the mortality rate caused by liver cancer was increasing 40% for men and 23% for women [1]. These rates are significantly higher than other cancer cases (most cases are decreasing).

Computed tomography (CT) is a medical imaging method using tomography. It generates a three dimensional image of the inside of an object (usually human body) from a large series of two-dimensional x-rays images taken around a single axis of rotation. The interaction of x-rays in a region of body varies with the energy of the photons and the effective atomic numbers and the electron density of the region. It is shown that the attenuation of x rays in tissue depends of the composition of the tissue. The difference of the electron density will be resulting in differences of intensity in CT images [2].

Liver and other surrounding organs have different electron density as show for example liver and pancreas as shown in Table 1.

**Table 1. Electron Density of Body Area [2]**

| Tissue | Electron Density (electrons/$cm^3$) |
|---|---|
| Water | $3.35 \times 10^{-23}$ |
| Bone | $3.72 – 5.29 \times 10^{-23}$ |
| Spleen | $3.52 \times 10^{-23}$ |
| Liver | $3.51 \times 10^{-23}$ |
| Heart | $3.46 \times 10^{-23}$ |
| Muscle | $3.44 \times 10^{-23}$ |
| Kidney | $3.42 \times 10^{-23}$ |
| Pancreas | $3.40 \times 10^{-23}$ |
| Fat | $3.07 \times 10^{-23}$ |
| Lung | $0.83 \times 10^{-23}$ |

The electron density difference is resulting in different intensity value of CT images as shown in Figure 1.

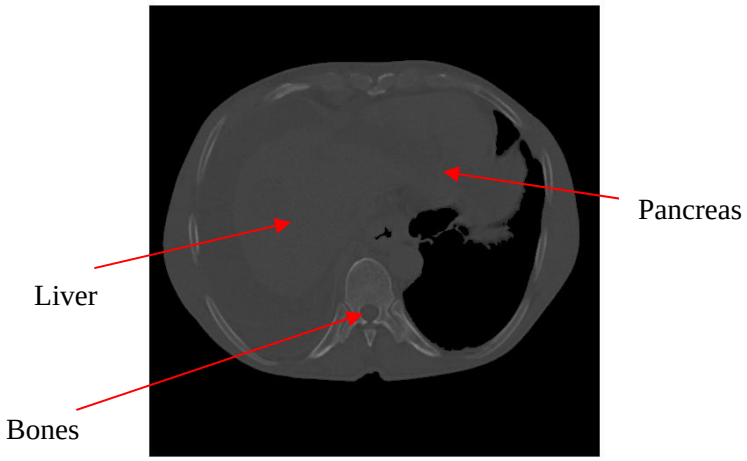


Figure 1. Different intensity of organs in CT images

In CT images, cancers located in a liver are generally identified by intensity difference between cancer and liver. Due to advent in computer technology, image processing technology has been used to assist physician in identifying cancer in liver [3, 4, 5, 6].

The intensity of the tumor can be lower and or higher than that of the liver. The main problem of liver cancer/ tumor detection is due to low contrast difference between cancer/ tumor and liver intensity values. Moreover, cancers/ tumors sometimes present in a very small region and thus make the detection even more difficult. Therefore, the objective of our work is to enhance contrast of CT image containing liver and tumor as a necessary preprocessing so that users are able to identify cancer/ tumor in CT images.

## 2 Approach

Instead of liver, several organs also exist in this CT image. The presence of these organs must be considered.

Since tumor is located inside the liver's area, it is important to identify the liver prior to detecting the tumor. The approach consists of two steps. Firstly, we concentrate on the segmentation of region of interest (i.e. liver and tumor). Secondly, in order to better visualize liver and tumor, the Region of Interest (ROI) is enhanced.

One of the widely used methods to enhance the contrast of an image is by manipulating histogram of the image. An example of liver tumor CT image and its histogram is shown in Figure 2. We found that the histogram of liver tumor CT image is bimodal. Histogram shows that the pixel distribution of liver and tumor is located in the right side of the histogram as indicated in red circle in Figure 2(b).

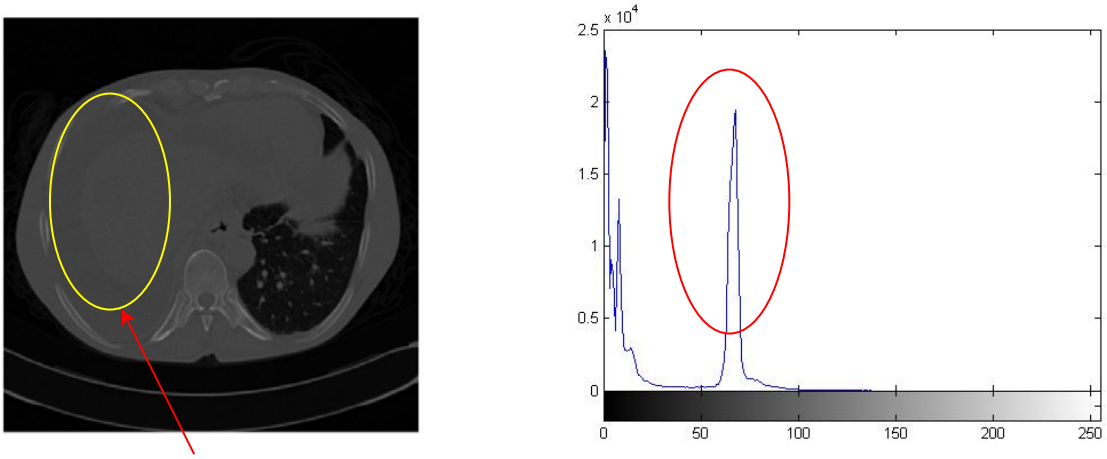


a. b.

Figure 2. (a) Liver tumor CT image, (b) Histogram of image (a)

Therefore, in order to segment the ROI, pixels that do not belong to the ROI (liver and tumor) are excluded. Since the histogram is bimodal, Otsu method is applied to exclude the unwanted pixels. Otsu's method works well on the image with bimodal histogram [7,8]. Otsu uses between-class variance as the measure of separability between classes [9]. Its definition, which follows bellow, utilizes histogram information derived from the input image.

Let $a$ be an input image and let $\bar{h}$ be the normalized histogram of $a$. The pixels of $a$ are partitioned into $k$ classes $C_0, C_1, \ldots, C_{k-1}$. The probability of class occurrence $\Pr(C_i)$ are given by,

$$\Pr(C_0) = \omega_0 = \sum_{j=0}^{\tau_1} \bar{h}(j) = \varpi(\tau_1)$$

$$\Pr(C_i) = \omega_i = \sum_{j=\tau_{i+1}}^{\tau_{i+1}} \bar{h}(j) = \varpi(\tau_{i+1}) - \varpi(\tau_1)$$

$$\Pr(C_{k-1}) = \omega_{k-1} = \sum_{j=\tau_{k-1}+1}^{l-1} \bar{h}(j) = 1 - \varpi(\tau_{k-1}) \tag{1}$$

here $\omega(\tau_1) = \sum_{j=0}^{\tau_1} \bar{h}(j)$ is the $0^{th}$-order cumulative moment of the histogram evaluated up to the $\tau_i$ th level. The class mean levels are given by,

$$\mu_0 = \sum_{j=0}^{\tau_1} \frac{j.\bar{h}(j)}{\omega_0} = \frac{\mu(\tau_1)}{\omega(\tau_1)}$$

$$\mu_i = \sum_{j=\tau_1+1}^{\tau_{i+1}} \frac{j.\bar{h}(j)}{\omega_i} = \frac{\mu(\tau_{i+1}) - \mu(\tau_i)}{\omega(\tau_{i+1}) - \omega(\tau_i)}$$

$$\mu_{k-1} = \sum_{j=\tau_{k-1}+1}^{l-1} \frac{j.\bar{h}(j)}{\omega_{k-1}} = \frac{\mu_r - \mu(\tau_{k-1})}{1 - \omega(\tau_{k-1})} \tag{2}$$

where $\mu(\tau_1) = \sum_{j=0}^{\tau_1} j.\bar{h}(j)$ is the $1^{st}$ order cumulative moment of the histogram up to the $\tau_i$ th level and $\mu = \sum_{j=0}^{l-1} j.\bar{h}(j)$ is the total mean level of $a$.

In order to evaluate the threshold value, the between class variance is used as discriminant measure of class separability. The between-class variance, $\sigma_b^2$, is defined as

$$\sigma_b^2 = \omega_0\mu_0^2 + \omega_1\mu_1^2 + ... + \omega_{k-1}\mu_{k-1}^2 - \mu^2 \tag{3}$$

The threshold value, $\tau$, is defined as the threshold value which optimize the between-class variance [8, 9].

Seo *et al* proposed histogram processing and histogram tail threshold to segment liver region by eliminating neighboring abdominal organs of the liver, such as the pancreas, spleen, and kidneys [10, 11]. In this work, we threshold the histogram undergoing Otsu's algorithm using the maximum ($\max_{ROI}$), minimum ($\min_{ROI}$), and the median ($\text{med}_{ROI}$) intensity of the ROI. The segmented ROI is shown in Figure 3.


Figure 3. (a) Segmented image with unnecessary region, (b) Region of interest

The white area shown in Figure 3(a) is related to the region of interest. However, this white area still contains unnecessary region for liver detection. Therefore, we consider only the region with the biggest area as the region of interest (Figure 3(b)).

In this work, the maximum ($max_{ROI}$) and minimum ($min_{ROI}$) intensity of the ROI are used to detect the location of the liver from the ROI. We stretch the intensity of the ROI by setting $max_{ROI}$ and $min_{ROI}$ as maximum (255) and minimum (0) intensity of the gray level (see Figure 4).

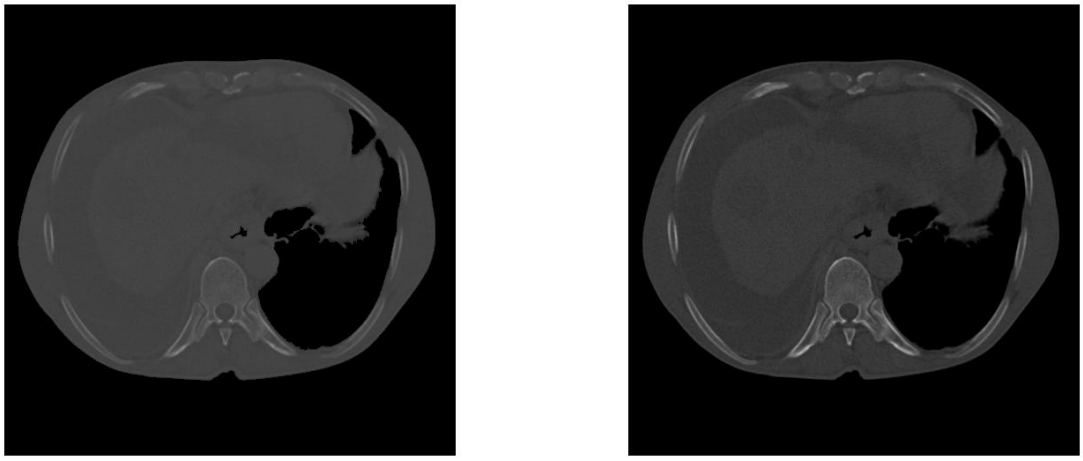

A B

Figure 4. (a) ROI from original image (b) Image (a) after contrast stretching

Having acquired the region of the liver, we subsequently enhance the contrast of pixel intensity in the region of interest containing liver and tumor to detect the tumor inside the liver area. From Figure 4(b), liver can be revealed; however, the tumor located inside the liver is not well identified. Therefore, we took samples of liver and tumor area from the several CT images (see Section 3) to determine average of intensity level of liver and tumor, respectively. These values are used as high input and low input for enhancing the contrast between the tumor and the liver as illustrated in Figure 5.

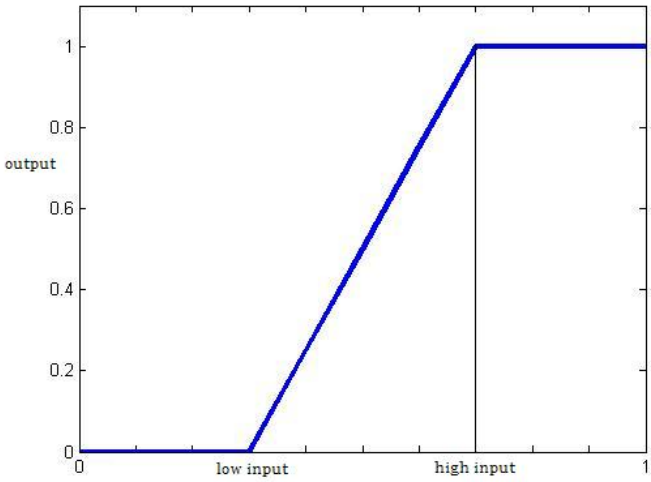


Figure 5. Intensity stretching for contrast enhancement

## 3 Result

The algorithm is applied on the CT images provided by the 3D liver tumor segmentation challenge 2008 website. The data set consists of 4 training images with 10 tumor reference images and 6 testing images. A liver tumor CT image data consists one 64-slice and two 40-slice acquired from CT scanners.

The four training images are used to determine the low input and high input for contrast enhancement (Figure 5). Figure 6(a) shows the region of interest taken from the original image. Intensity stretching is used to enhance the contrast of this image and result is shown in Figure 6(b).

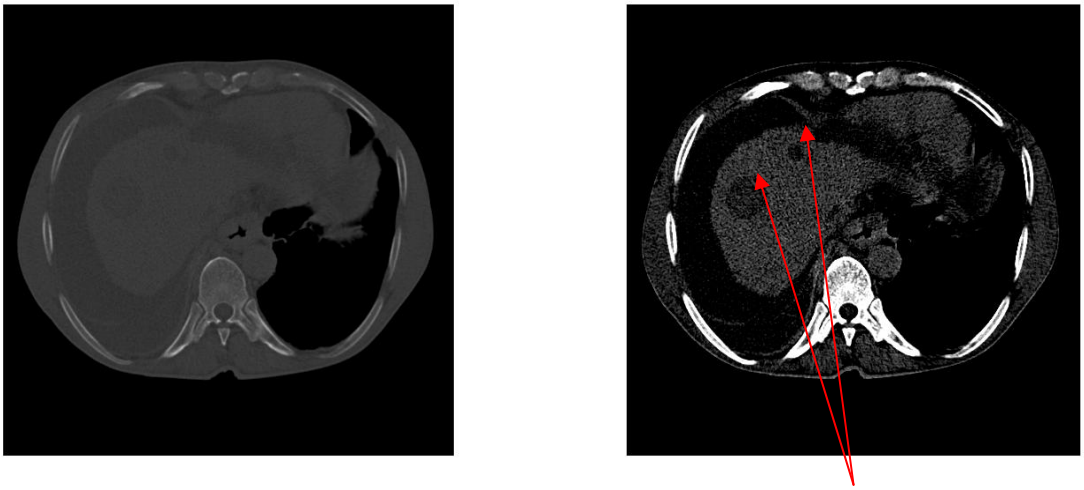


A B

Figure 6. (a) ROI showing liver area, (b) Image (a) after contrast enhancement showing tumor inside the liver.

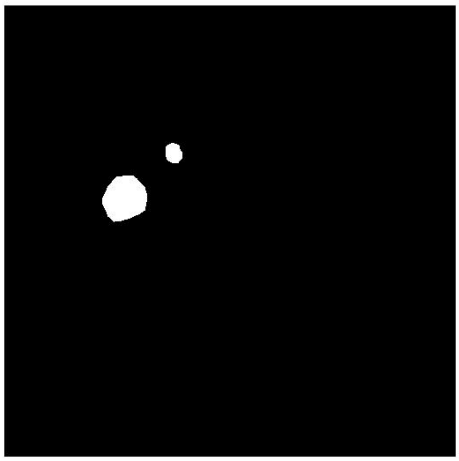

Figure 7. The two segmented tumors of Figure 6(b) shown in the white area

**Table 2. Performance of Proposed Method**

| | Overlap Error | | Volume Difference | | Ave. Surf. Dist. | | RMS Surf. Dist. | | Max. Surf. Dist. | | |
|---|---|---|---|---|---|---|---|---|---|---|---|
| Tumor | (%) | Score | (%) | Score | (mm) | Score | (mm) | Score | (mm) | Score | Total Score |
| IMG05_L1 | 27.44 | 79 | 3.31 | 97 | 1.89 | 52 | 2.63 | 63 | 11.55 | 71 | 72 |
| IMG05_L2 | 35.56 | 73 | 28.19 | 71 | 1.39 | 65 | 2.08 | 71 | 9.95 | 75 | 71 |
| IMG05_L3 | 44.07 | 66 | 27.90 | 71 | 1.82 | 54 | 2.50 | 65 | 7.50 | 81 | 67 |
| IMG06_L1 | 31.32 | 76 | 20.76 | 78 | 0.80 | 80 | 1.19 | 83 | 6.95 | 83 | 80 |
| IMG06_L2 | 37.80 | 71 | 2.04 | 98 | 0.86 | 78 | 1.27 | 82 | 6.37 | 84 | 83 |
| IMG07_L1 | 29.86 | 77 | 11.24 | 88 | 4.76 | 0 | 7.99 | 0 | 41.32 | 0 | 33 |
| IMG07_L2 | 30.74 | 76 | 14.27 | 85 | 1.42 | 64 | 1.86 | 74 | 7.12 | 82 | 76 |
| IMG08_L1 | 18.54 | 86 | 15.47 | 84 | 1.99 | 50 | 2.60 | 64 | 10.68 | 73 | 71 |
| IMG09_L1 | 27.70 | 79 | 17.32 | 82 | 0.92 | 77 | 1.45 | 80 | 8.23 | 79 | 79 |
| IMG10_L1 | 29.09 | 78 | 17.12 | 82 | 1.60 | 60 | 2.06 | 71 | 7.60 | 81 | 74 |
| Average | 31.21 | 76 | 15.76 | 84 | 1.75 | 58 | 2.56 | 65 | 11.73 | 71 | 71 |

There are five parameters to measure the performance of the proposed methods, namely, volumetric overlap error, volume difference, average surface distance, RMS surface distance and maximum surface distance [12]. Volumetric overlap error shows the number of voxels in the intersection of segmentation and reference, divided by the number of voxels in the union of segmentation and reference. Relative absolute volume difference shows the total volume of the segmentation is divided by the total volume of the reference. Using the proposed method, we obtain average error of 31.21 % volumetric overlap and 15.76% relative absolute volume different. These error percentages are predicted due to accumulative error of each slice.

Moreover, average symmetric absolute surface distance which is related to voxels in the object that have at least one neighbour (from the 26 nearest neighbours) that does not belong to the object is used to determine the border voxels of segmentation and reference. Symmetric root mean square (RMS) surface distance is similar to the previous measure, but stores the squared distances between the two sets of border voxels. Results show that from the six test CT images with possible ten indicated tumors, we obtain 1.75 mm and 2.56 mm for average symmetric absolute surface distance and RMS surface distance, respectively. Eventually, maximum symmetric absolute surface distance of 11.73 is obtained to show the maximum of all voxel distances. Perfect segmentation is represented by 0 for the average symmetric absolute surface distance, RMS symmetric surface distance and maximum symmetric absolute surface distance. Based on this reference, the proposed method is able to significantly enhance the contrast

between the liver and tumor and results in relatively accurate identification of the existing tumors.

## 4 Conclusion

Identification of a liver tumor from CT images is challenging due to the very low contrast between the tumor and the liver. The presence of other organs having similar intensity level and various dimensions makes the tumor detection even more difficult. In this work, we use histogram manipulation to both segment the region of interest containing liver and tumor and enhance the contrast of the tumor and liver from CT images. The proposed method can successfully enhance the contrast of the liver tumor in CT images so that the tumor can be identified from the liver.

## Reference

[1] A. Jemal, R. Siegel, E. Ward, T. Murray, J. Xu and M.J. Thun. *Cancer Statistics, 2007*. CA Cancer J Clin 2007; 57;43-66.

[2] W. R. Hendee and E.R. Ritenour. *Medical Imaging Physics*. Wiley-Liss Inc, New York 2002.

[3] E.L. Chen, P.C Chung, C. L. Chen, H. M. Tsai and C-I Chang. *An Automatic Diagnostic System for CT Liver Image Classification*. IEEE Transactions on Biomedical Engineering 1998; 45.

[4] F. Bin, W. Hsu and L. Mong Li. *On the Accurate Counting of Tumor Cells*. IEEE Transactions on Bioscience 2003;2; 94-103.

[5] G. Glombitza, W. Lamade, A. M. Demiris, M.R Gopfert, A. Mayer, M. L Bahner , H.P Meinzer, G. Ritchter, T. Lehnert and C. Herfarth. *Virtual Planning of Liver Resections:Image Processing, Visualization and Volumetric Evaluation*. International Journal of Medical Informatics 1999; 53; 225.

[6] K. Mala and V. Sadasivam. *Wavelet based Texture Analysis of Liver Tumor from Computed Tomography Images for Characterization Using Linear Vector Quantization Neural Network*. International Conference on Advanced Computing and Communications 2006; 267-270.

[7] R. C. Gonzales and R. E. Woods. *Digital Image Processing*. Addison-Wesley Longman Publishing 1992.

[8] G. X. Ritter and J. N. Wilson. *Handbook of Computer Vision Algorithms in Image Algebra*. CRC Press 2000.

[9] N. Otsu. *A Threshold Selection Method from Gray-Level Histograms*. IEEE Transactions on Systems, Man, and Cybernetics 1979; 9; 62-66

[10] K.S. Seo.*Improved Fully Automatic Liver Segmentation Using Histogram Tail Threshold Algorithms*. Computational Science – ICCS 2005; 822.

[11] K.S. Seo, H. B. Kim, T. Park, P. K. Kim and J. A. Park. *Automatic Liver Segmentation of Contrast Enhanced CT Images Based on Histogram Processing*. Advances in Natural Computation. 2005; 1027.

[12] Gerig, M. & Chakos, M. Valmet. *A new validation tool for assessing and improving 3D object segmentation*. MICCAI 2001. Springer, Berlin 2001; 516-523.